

**DERIVATIZED GUAR GUMS BASED
HYDROGEL FILM AS CARRIER FOR
PIROXICAM**

Thesis Submitted

in Partial Fulfilment of the Requirements for the

Degree of

MASTER OF SCIENCE

In

CHEMISTRY

By

SYED RIZWAN ALI

(2K22/MSCCHE/42)

Under the Supervision of

Prof. ARCHNA RANI



Department of Applied Chemistry

DELHI TECHNOLOGICAL UNIVERSITY

(formerly Delhi College of Engineering)

Shahbad Daultpur, Main Bawana Road, Delhi-110042, India

May, 2024



DELHI TECHNOLOGICAL UNIVERSITY
(formerly Delhi College of Engineering)
Shahbad Daultapur, Main Bawana Road, Delhi-110042, India

CANDIDATE'S DECLARATION

I, Syed Rizwan Ali (2k22/MSCCHE/42) hereby certify that the work which is being presented in the dissertation enlightened “**Derivatized Guar Gum based Hydrogel Films as a Carrier for Piroxicam**” in partial fulfilment of the requirements for the award of the Degree of Master in Science, submitted in the Department of Applied Chemistry, Delhi Technological University is an authentic record of my own work carried out during the period from June 2023 to April 2024 under the supervision of Prof. Archana Rani.

The matter presented in the dissertation has not been submitted by me for the award of any other degree of this or any other institute.

DATE: 31-05-2024

Syed Rizwan Ali
(2K22/MSCCHE/42)



DELHI TECHNOLOGICAL UNIVERSITY
(formerly Delhi College of Engineering)
Shahbad Daultapur, Main Bawana Road, Delhi-110042, India

CERTIFICATE BY THE SUPERVISOR

Certified that Syed Rizwan Ali (2k22/MSCCHE/42) has carried out her research work presented in this dissertation entitled “**Derivatized Guar Gum based Hydrogel Films as a Carrier for Piroxicam**” for the award of Master of Science from the Department of Applied Chemistry, Delhi Technological University, Delhi, under my supervision. The dissertation embodies results of original work, and studies are carried out by the student himself and the contents of the dissertation do not form the basis for the award of any other degree to the candidate or to anybody else from this or any other University/Institution.

Prof. ARCHNA RANI

Professor

Department of Applied Chemistry

Date: 31-05-2024

ACKNOWLEDGEMENT

The success and outcome of this project required a lot of guidance and assistance from many people and I am extremely fortunate to have got this all along the completion of this project work.

I would like to express my gratitude towards my project supervisor, Prof. Archana Rani, Department of Applied Chemistry, Delhi Technological University, for their individual guidance and support throughout the research project and work under their able guidance.

I am thankful for and fortunate enough to get constant encouragement, support, and guidance from Mrs. Meenakshi Tanwar, who helped me in completing my project work. Her constant support and willingness to share valuable information has enhanced my learning throughout the subject matter.

I would also like to thank the teaching staff and lab staff of Delhi Technological University whose assistance and cooperation have been integral to the successful completion of my dissertation project.

Finally, yet importantly, I would like to express my heartfelt thanks to my beloved family and friends who have endured my long working hours and whose motivation kept me going. Thank you for all of your support and patience in helping guide me through the good time and bad.

SYED RIZWAN ALI

OBJECTIVE

- Synthesis of Hydrogel Films using Hydroxypropyl Guar Gum and Carboxymethyl Guar Gum using Citric Acid as a crosslinker.
- Fabrication of Piroxicam loaded film to use them as innovative carrier drug delivery systems.
- Structural Characterization of hydrogel film such as Attenuated Total Reflection - Fourier Transform Infrared Spectroscopy (ATR-FTIR) and X-Ray Diffraction (XRD).
- Morphological Characterization of hydrogel film using Field Emission Scanning Electron Microscopy (FE-SEM).
- Thermal Characterization of hydrogel film using Thermogravimetric Analysis (TGA).
- Rheological Characterization of the hydrogel solution to access the viscoelastic properties and flow behaviour of the film
- To access the Drug Release Kinetics of the Piroxicam loaded film in Phosphate Buffer (pH = 7.4)

ABSTRACT

A recent study has been performed on making hydrogel films with hydroxypropyl guar gum and carboxymethyl guar gum crosslinked with citric acid. The crosslinking of HyPGG, CaMGG, and CTA into a film-like structure was achieved through a crosslinked network structure. Due to their biocompatibility and biodegradability, both HyPGG and CaMGG have the potential to be used as hydrogel films for drug delivery systems. The research revealed that, the drug carrier CaMGG-based hydrogel, syntheses have exhibited noticeable viscoelastic properties, surface morphology, and thermal behaviour. On the other hand, HyPGG has been applied in initial studies creating network hydrogel platforms designed for drug delivery that could present a combination of local drug delivery properties in combination with biological compatibility. The customized drug release features of both derivatives make them suitable for targeted drug delivery applications in pharmaceutical and biomedical fields.

The use of crosslinker as citric acid has been discussed in various compositions of citric acid crosslinked hydrogel films in several research studies. Previous inquiries have suggested that the citric acid could be used as crosslinker and were found to improve the properties of hydrogel that produced from natural polymer. The use of citric acid in hydrogels enhances water resistant properties, and had better mechanical and physical properties. Due to its biocompatibility, citric acid can form ester bonds and it is environmentally safe, which has played a significant importance in making the films of this hydrogel could be applied on tissue engineering and wound treatment.

Thus, the investigation of the synthesized hydrogel film was carried out using different characterization methods. Thermogravimetric Analysis (TGA) was used to study the thermal decomposition of the hydrogel film. The structural properties were investigated by ATR-FTIR (attenuated total reflection -Fourier Transform Infrared Spectroscopy) and XRD (X-ray Diffraction). Field Emission Scanning Electron Microscope (FE-SEM) has been performed onto hydrogel film for morphological examination. The viscoelastic behaviour of hydrogel film was evaluated by rheological analysis. The prepared hydrogel films incorporated with Piroxicam was as a vehicle

for advanced drug delivery system. The hydrogel film's in vitro drug release was studied in PBS 7.4. The HyPPG-co-CaMGG-cl-CTA hydrogel film followed Korsmeyer-Peppas model and followed Fickian diffusion in pH 7.4. This shows potential of the hydrogel film to act as a carrier for innovative drug delivery systems.

KEYWORDS:

Hydroxypropyl Guar Gum, Carboxymethyl Guar Gum, Citric Acid, hydrogel films, Piroxicam, PBS 7.4, Korsmeyer-Peppas, Fickian diffusion

CONTENTS

TITLE	PAGE NUMBER
Candidate Declaration	i
Certificate	ii
Acknowledgement	iii
Objective	iv
Abstract	v
CHAPTER 1: Introduction and Literature Review	2
CHAPTER 2: Materials, Synthesis & Characterization	
2.1: Materials	9
2.2: Methods Involved	9
2.3: Characterization	10
CHAPTER 3: Results and Discussion	
3.1: FTIR	18
3.2: XRD	19
3.3: SEM	21
3.4: TGA	22
3.5: Rheological Analysis	24
3.6 Swelling Studies	27
CHAPTER 4: Drug Delivery Application	30
Conclusion	33
References	34

LIST OF FIGURES

Figure 1.1: Guar Gum and its Derivatives

Figure 1.2: Structure of Hydroxypropyl Guar Gum

Figure 1.3: Structure of Carboxymethyl Guar Gum

Figure 1.4: Structure of Citric Acid

Figure 1.5: Structure of Piroxicam

Figure 2.1: Fabrication of HyPPG-*co*-CaMGG-*cl*-CTA

Figure 2.2: Perkin-Elmer Spectrum Two L160000A FTIR Spectrophotometer

Figure 2.3: Perkin Elmer TGA 4000

Figure 2.4: Zeiss GeminiSEM 500 Field Emission Scanning Electron Microscope

Figure 2.5: X'Pert Pro MRD Pananalytical X-Ray Diffractometer

Figure 2.6: Anton Paar Modular Compact Rheometer 302

Figure 2.7: Folding Axes of the Hydrogel Film for Folding Endurance

Figure 3.1: FTIR Spectra of HyPPG, CaMGG & Hydrogel film

Figure 3.2: XRD Spectra of HyPPG, CaMGG, CTA & Hydrogel Film

Figure 3.3: Scanning Electron Micrographs of HyPPG, CaMGG & Hydrogel Film

Figure 3.4: Thermogravimetric Analysis of HyPPG, CaMGG & Hydrogel Film

Figure 3.5: Rheological Studies of hydrogel film solution

Figure 3.6: Swelling Studies

Figure 4.1: Release Kinetics of the Hydrogel Film

LIST OF ABBREVIATIONS

- HyPGG – Hydroxypropyl Guar Gum
- CaMGG – Carboxymethyl Guar Gum
- CTA – Citric Acid
- PXM – Piroxicam
- FT-IR – Fourier Transform Infrared Spectroscopy
- TGA – Thermogravimetric Analysis
- XRD – X-Ray Diffraction
- SEM – Scanning Electron Microscopy
- *-co-* – Co-polymerization
- *-cl-* – Crosslinking
- PBS – Phosphate Buffer

LIST OF TABLES:

TABLE 2.1: Optimization of Synthesis Reaction and Folding Endurance

TABLE 3.1: Swelling Ratio of different formulations by varying CTA

TABLE 4.1: Drug Release Kinetics of Piroxicam loaded Hydrogel Film

CHAPTER 1
INTRODUCTION &
LITERATURE SURVEY

With the unfolding of intricacies in the recent exploration and researches, Gums are used as a disintegrant in pharmaceutical drug delivery applications. This field has perceived a notable change towards the advancement of improved drug delivery system by the virtue of its pervasive accessibility, non-toxic attributes and economically justified production costs.[1] They are also being investigated for their potential applications in drug delivery, across a spectrum of applications such as in drug delivery systems, in a wide array of therapeutic blends such as hydrogels[2], nanoparticles[3], microspheres[4], suspension stabilizers[5], etc. Abundantly present in the natural realm, natural gums boast a spectrum of attributes such as their viscous nature, adhesive constitution, and biocompatibility, making them absolute choices for drug delivery applications. Moreover, natural gums offer advantages such as controlled drug release, increased stability of drugs, and enhanced bioavailability.

Natural gums such as plant and polysaccharide-derived gums are high molecular weight complex polymers, containing a wide range of sugar units, including glucose, galactose, rhamnose, arabinose, mannose and uronic acids. These gums have diverse sources like coming from plant seeds such as gums from locust bean & guar, exudates like acacia & tragacanth gums, microbial sources such as xanthan & gellan gum, mucilage like psyllium gum, seaweed varieties including alginate & carrageenan and animal polysaccharides like chitin & chitosan[6]. They have attracted significant interest among researchers for the creation of three-dimensional cross-linked structures known as hydrogels, which serve as foundational materials in various pharmaceutical applications. This is because these natural raw materials will continue to be accessible in the immediate future. The unique properties of natural gums, such as their ability to decrease interfacial tension and undergo easy chemical modifications, make them suitable for the preparation of hydrogels and further used in drug delivery systems. Modifications in natural gums have been beneficial to various problems like non-uniform hydration rates, non-uniform viscosity build-up, drop of viscosity on storage, microbial contamination and so on. The prevalent safety of natural gums for consumption contributes to their extensive utilization in drug delivery and as food additives.[7]

Guar Gum, also known as Cyamopsis gum, Guaran, Guyan, Guarina, or Glucotard, is derived from seeds of *Cyamopsis tetragonolobus* and is a water-soluble and non-ionic polysaccharide of the Leguminosae family.[8] It is a hydrophilic polymer of alternating chains of (1→4)-d- methyl- α -d-glucopyranosyl linked to (1→6)-d-galactopyranosyl units. Guar gum gathers around 80% of galactomannan, 12% of water, 5% of protein, 2% of acidic insoluble ash and trace of fat. It is also used as a binding agent, disintegrant, suspension agent, thickening agent and stabilizer in the pharmaceutical field.[9] Its ability to thaw in cold water allows it to quickly form viscous pseudo plastic solutions with consistent viscosity and stability across various pH levels due to its non-ionic nature. However, the use of pure guar gum has sometimes been hindered by its uneven hydration rate, decreased viscosity over time, poor thermal stability and vulnerability to microbial contamination. To overcome these challenges, chemical modification of guar gum has become a valuable option because it offers a valuable solution to adjust the physiochemical properties of the resulting polymer according to specific application needs. With this reference, Hydroxypropyl Guar Gum (HyPGG) and Carboxymethylated Guar Gum (CaMGG) have emerged as exciting and versatile functional derivatives with great potential and wide range of applications.

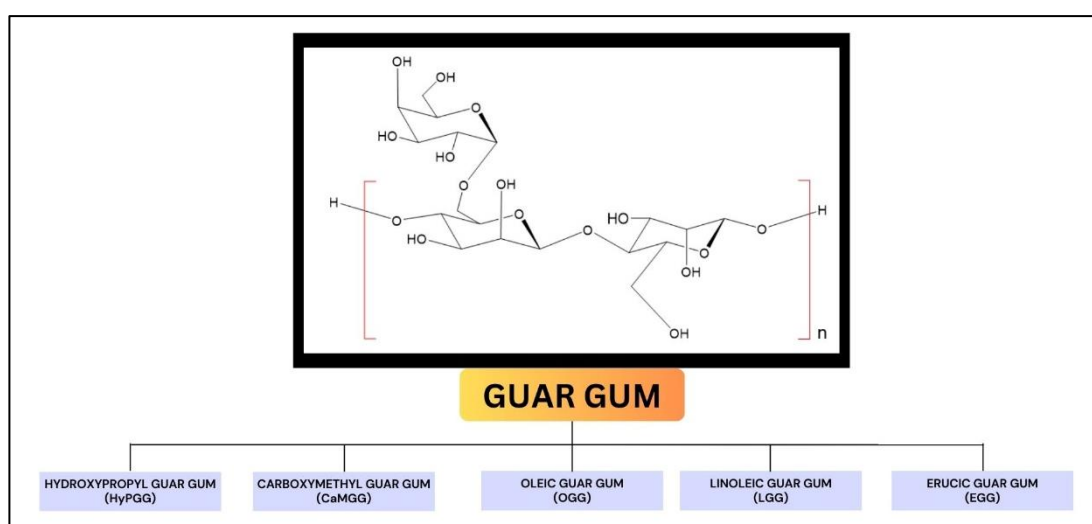


Figure 1.1: Prominent Derivatives of Guar Gum

Hydroxypropyl Guar Gum is a major step forward, with a wide range of industrial uses with its improved physical and chemical properties. HyPGG, a derivative of guar gum is created through an etherification reaction with propylene oxide. It offers superior dissolution rate, lower water insoluble content and enhanced stability compared to the traditional guar gum. The incorporation of hydroxypropyl moieties significantly modulates the rheology of guar gum, imparting a more robust and versatile thickening agent profile. HyPGG demonstrates superior emulsifying and stabilizing attributes, resulting to the increased density of hydroxypropyl groups that facilitate augmented hydrogen bonding with water molecules.[10] This modification translates to a reduction in polymer chain size and consequently a lower intrinsic viscosity, while preserving substantial thickening efficacy. Due to its higher solubility and lower viscosity than the original guar gum, it facilitates 1,3-hydroxyl substitution. HyPGG's thermal stability surpasses that of unmodified guar gum, rendering it an indispensable additive in high-temperature processes such as hydraulic fracturing[10]. Furthermore, its film-forming ability has been leveraged in the cosmetic industry[11].

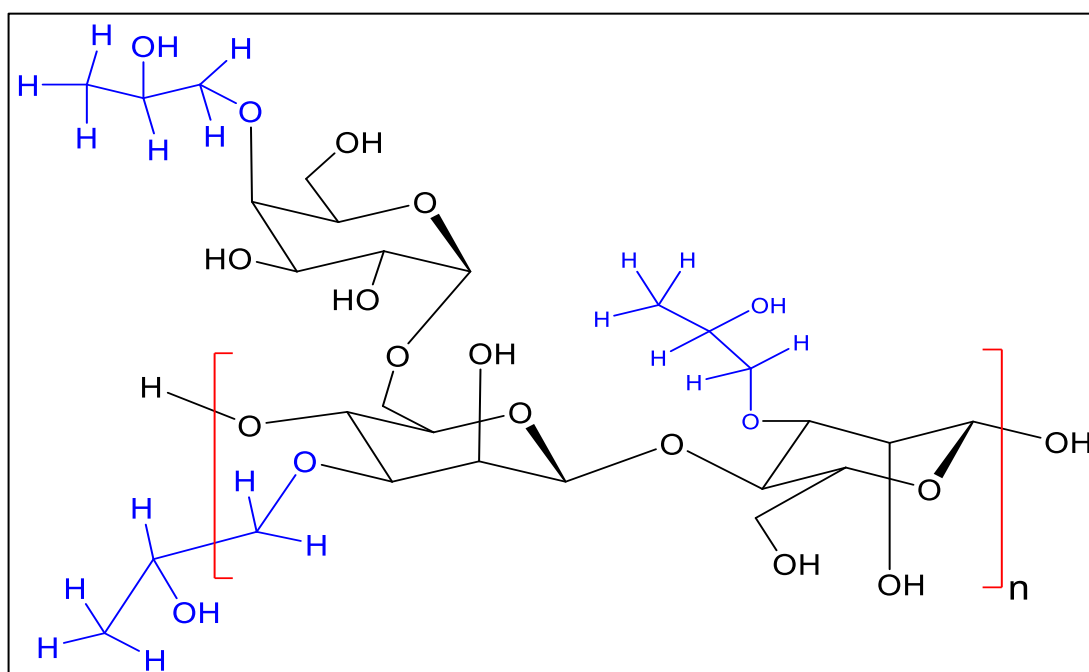


Figure 1.2: Structure of Hydroxypropyl Guar Gum

Carboxymethyl Guar Gum is another significant derivative of guar, offering enhanced physiochemical properties that are ideal for a variety of industrial applications. Carboxymethylation of the native guar gum is done through the reaction of the original gum with chloroacetic acid or its sodium salt followed by the activating the product with aq. NaOH in a mixture of an organic solvent[12]. This method is considered a suitable chemical approach for linking pendant carboxylic acid groups to pure guar gum because of its technical simplicity and wide-ranging applications. The emergence of CaMGG has significantly expanded the potential utilization of the native Guar Gum, offering improved solubility and stability compared to the parent polymer. The presence of carboxyl and hydroxy groups in the backbone of CaMGG allows for a diverse range of chemical reactions, enabling blending, crosslinking, copolymerization or grafting with other polymers or molecules of interest, thereby broadening the spectrum of applications[13]. Carboxymethylation has been reported to enhance water solubility and increase solution's viscosity, reducing biodegradability and thus, extending the shelf life compared to the original polysaccharide[14].

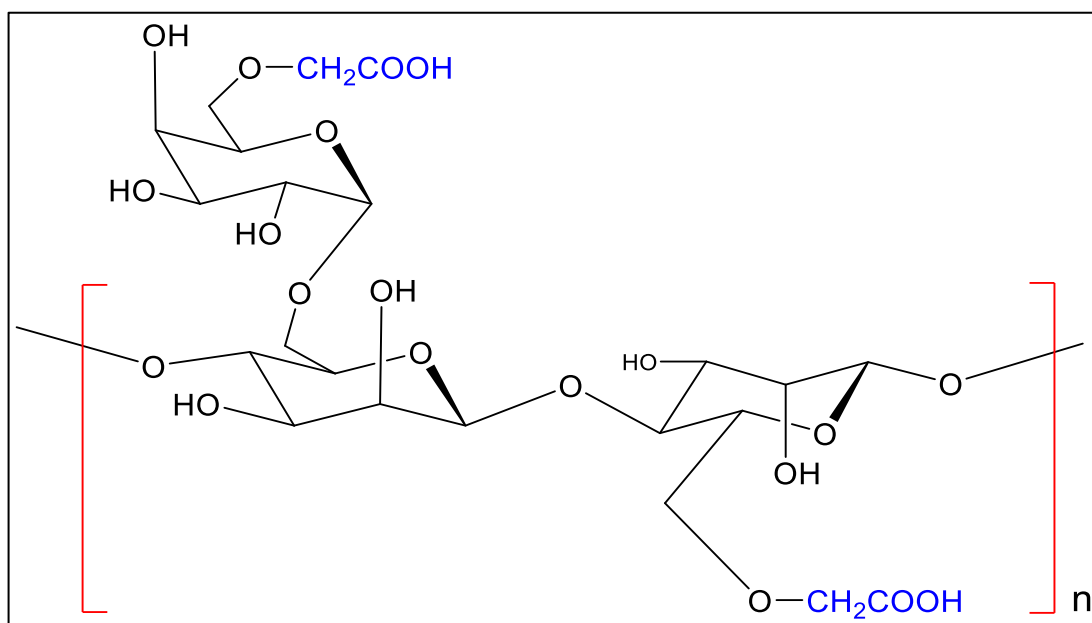


Figure 1.3: Structure of Carboxymethyl Guar Gum

Crosslinking water-soluble natural polymers like HyPPG and CaMGG with poly(carboxylic acid) such as Citric Acid (CTA) shows promise for modifying their nanocomposites. Citric acid (CTA), an organic acid with three carboxylic groups is present in many fruits particularly lemons and oranges. It is considered as non-toxic and serves as a popular natural additive in the food industry because of its preservative capabilities. This acid has shown evidence of being able to connect to hydroxyl groups at elevated temperatures ranging from 150°C to 160°C. In addition, it can function as a plasticizer at certain concentrations due to its simple reaction mechanism and ready availability as a non-toxic chemical[15]. Furthermore, by reacting it with hydroxyl-bearing biopolymer chains under mild conditions, citric acid significantly enhances mechanical properties while providing greater stability. This results in the formation of a steady matrix formation with increased swelling ability, thermal constancy and great resistance to water dissolution[16]. The crosslinking vitally occurs through interaction between the hydroxyl groups present in these guar gum derivatives enhancing hydrogen bonding interactions amid the polymer units. Thus, cross-linking emerges as an effective alternative for improving film properties derived from biopolymers.

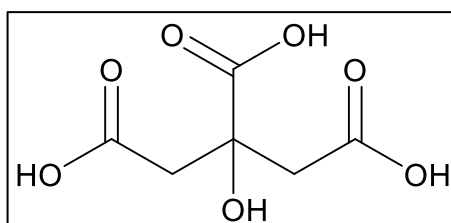


Figure 1.4: Structure of Citric Acid

Piroxicam (PXM) is classified under Class II in the Biopharmaceutics Classification System and is a medication with analgesic, antipyretic and anti-inflammatory properties. It is a Non-Steroidal Anti-Inflammatory Drug (NSAID) and has demonstrated effectiveness in treating osteoarthritis, chronic and acute rheumatoid arthritis, as well as postoperative conditions. This drug exhibits low water solubility at normal body pH levels. By reducing the number of polymorphnuclear cells in the joint fluid, it provides anti-inflammatory effect. Oral administration may lead to potential gastrointestinal mucosa ulceration side effects. Therefore, utilizing it as a drug-carrier patch of piroxicam could offer a safer alternative to tablets for addressing this concern.

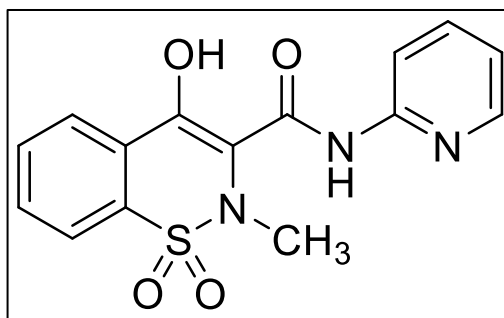


Figure 1.5: Structure of Piroxicam

This study describes the fabrication of HyPGG-co-CaMGG-cl-CTA hydrogel films containing *in-situ* loaded Piroxicam (PXM). This hydrogel exhibit pH-dependent and controlled release properties for Piroxicam (PXM). The hydrogels were analysed using ATR-FTIR, XRD, FE-SEM, TGA and ¹³C-NMR Solid State (SS). Furthermore, an extensive study of the kinetics of Drug Release was conducted employing diverse models such as Zero-Order model, Hixon-Crowell, Higuchi model, Korsmeyer-Peppas and First Order.

CHAPTER 2
MATERIALS, SYNTHESIS &
CHARACTERIZATION

2.1. MATERIALS REQUIRED

CaMGG powder was bought from local market, while HyPGG was obtained from Hindustan Pvt. Ltd. CA was acquired from CDH in New Delhi, Glycerol was sourced from Fisher Chemicals in the UK. Piroxicam was acquired from Laborate Pharmaceuticals Pvt. Ltd., Panipat. Milli-Q water was used for all experimental procedures.

2.2. METHODS INVOLVED

2.2.1 Synthesis of Control (HyPGG-co-CaMGG-cl-CTA) Film:

HyPGG-co-CaMGG-cl-CTA hydrogel films were created using the Solvent casting method. 0.2g of HyPGG and 0.2g of CaMGG were dissolved together in 60ml of Milli Q water at a ratio of 1:1 and mixed on a magnetic stirrer at 450 rpm for 2 hours until a uniform mixture was achieved. Citric Acid was then added as a crosslinker to the solution, with the gums-to-citric acid ratio maintained at 1:0.6 (R4). Additionally, 0.5 ml of Glycerol were incorporated as a plasticizer into the homogeneous solution, which was stirred for 12 hours until thoroughly mixed. The resulting solution underwent oil curing for 10 mins at 120°C before being sonicated for air bubble removal for half an hour. Subsequently, the final solution obtained was then transferred into Petri dishes and subjected to 60°C in an oven for about 24 hours to facilitate drying. The dried product obtained from this process served as the material from which subsequent film analysis could be carried out.

2.2.2 Synthesis of PXM loaded R4 Film:

Hydrogel film containing PXM was produced following the same procedure. Except 7mg of PXM thawed in 14 ml ethanol was added to the homogenized solution of HyPGG, CaMGG, CTA and glycerol and stirred for 12 hours until a uniform mixture was achieved. The final solution was transferred into a petri dish and subjected to 60°C for 24 hours in an oven to facilitate drying, creating the drug-loaded hydrogel film.

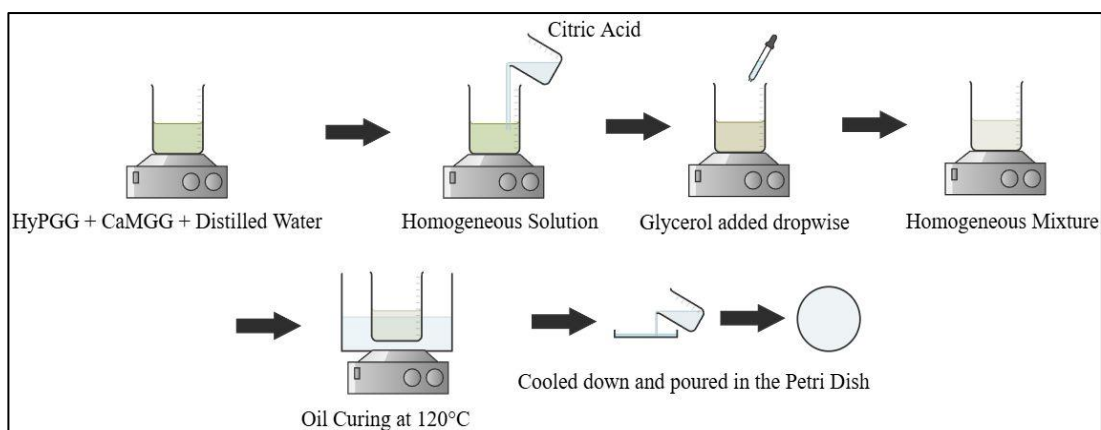


Figure 2.1: Fabrication of HyPGG-co-CaMGG-cl-CTA

2.3. CHARACTERIZATION OF HyPGG, CaMGG & HyPGG-co-CaMGG-cl-CTA FILM:

2.3.1 Attenuated Total Reflection - Fourier Transform Infrared Spectroscopy (ATR-FTIR)

Study of the functional groups in HyPGG, CaMGG, and HyPGG-co-CaMGG-cl-CTA was conducted using the Perkin-Elmer Spectrum Two L160000A FT-IR at room temperature. The data were gathered in the range of 4000-400 cm^{-1} .

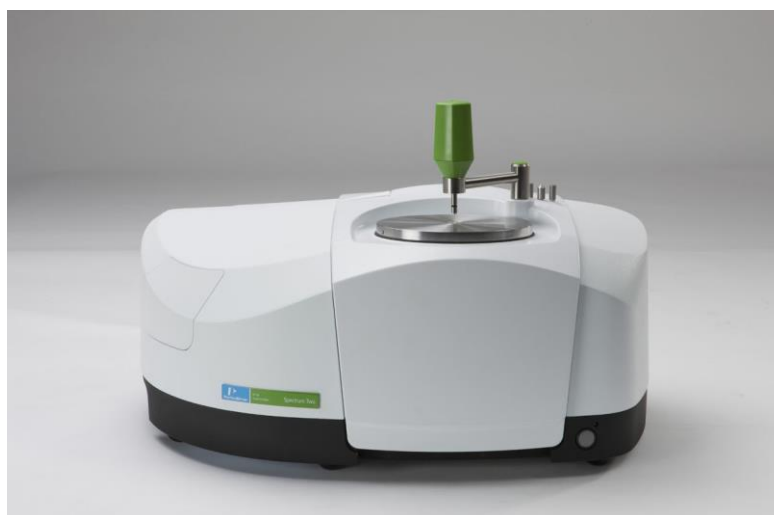


Figure 2.2: Perkin-Elmer Spectrum Two L160000A Fourier Transform Infrared Spectrophotometer

2.3.2 Thermogravimetric Analysis (TGA)

The thermal constancy of the HyPPG, CaMGG, and HyPPG-co-CaMGG-cl-CTA film was assessed using thermogravimetric analyser, Perkin Elmer, TGA 4000. The samples were heated from 25°C to 800°C at a rate of 10°C/min under an N₂ atmosphere within a platinum crucible.



Figure 2.3: Perkin Elmer TGA 4000

2.3.3 Field Emission Scanning Electron Microscopy (FE-SEM)

The morphological and physical characteristics of HyPPG, CaMGG, and HyPPG-co-CaMGG-cl-CTA were analyzed using a Zeiss GeminiSEM 500 Field Emission Scanning Electron Microscope at magnifications of 500, 1000, and 2000 with a fast-tracking high voltage (HV) of 10 kV and working distance (WD) at 10.3 millimeters.



Figure 2.4: Zeiss GeminiSEM 500 Field Emission Scanning Electron Microscope

2.3.4 X-ray Diffraction (XRD)

To acquire vital insights into the solid-state arrangement of HyPGG, CaMGG, and the HyPGG-*co*-CaMGG-*cl*-CTA film, we utilized a Pananalytical X-ray diffractometer (X'pert Pro MRD). The analysis employed Cu-K α radiations with a wavelength of 1.540598 Å within a scanning range of 2θ (1.5°-80.02°) and at a scan rate of 1°/min. These extents were carried out at 20 kV and with a current of 10 mA.



Figure 2.5: X'Pert Pro MRD Pananalytical X-Ray Diffractometer

2.3.5 Rheological Analysis

The Anton Paar Modular Compact Rheometer 302 was utilized to analyze the rheological characteristics of the HyPPG-*co*-CaMGG-*cl*-CTA film at ambient room temperature. The testing was carried out with a 40mm parallel plate setup.



Figure 2.6: Anton Paar Modular Compact Rheometer 302

2.3.6 Swelling Studies

The films were trimmed into consistent sizes, each weighing 0.1g. Subsequently, each film was submerged in 10 millilitres of Phosphate buffer (pH = 7.4 at ambient room temperature). It was then monitored at specific time intervals - first observed every 30 minutes for a duration of 6 hours and finally after 24 hours had elapsed. After the immersion phase, the hydrogel films were taken out of the phosphate buffer and then weighed after removing any remaining buffer solution by gently dabbing with a tissue paper. The swelling experiments were conducted three times to ensure accuracy.

To evaluate the hydrogel films' swelling behaviour, they were submerged in Phosphate Buffer 7.4 and their weight changes over time were measured using the equation:

$$\text{Swelling Index (\%)} = \frac{W_s - W_d}{W_d} \times 100$$

W_d = weight of dried hydrogel film

W_s = weight of swollen hydrogel film.

2.3.7 Impact of CTA on hydrogel film, Thickness and Folding Endurance:

The thickness of HyPGG-*co*-CaMGG-*cl*-CTA hydrogel film was recorded as 0.7500 mm using Vernier Callipers having a diameter of 103 mm.

TABLE 2.1: Impact of CTA on hydrogel film and their Folding Endurance

Sample Code	HyPGG (gm)	CaMGG (gm)	CTA (gm)	Glycerol	Ratio (Gums:CTA)	Folding Endurance
R1	0.2	0.2	0	0	1:0	None
R2	0.2	0.2	0.08	0.5 ml	1:0.2	1
R3	0.2	0.2	0.16	0.5 ml	1:0.4	6
R4	0.2	0.2	0.24	0.5 ml	1:0.6	8
R5	0.2	0.2	0.32	0.5 ml	1:0.8	3
R6	0.2	0.2	0.4	0.5 ml	1:1	2
R7	0.2	0.2	0.48	0.5 ml	1:1.2	2
R8	0.2	0.2	0.56	0.5 ml	1:1.4	1
R9	0.2	0.2	0.64	0.5 ml	1:1.6	1
R10	0.2	0.2	0.72	0.5 ml	1:1.8	1
R11	0.2	0.2	0.80	0.5 ml	1:2	1

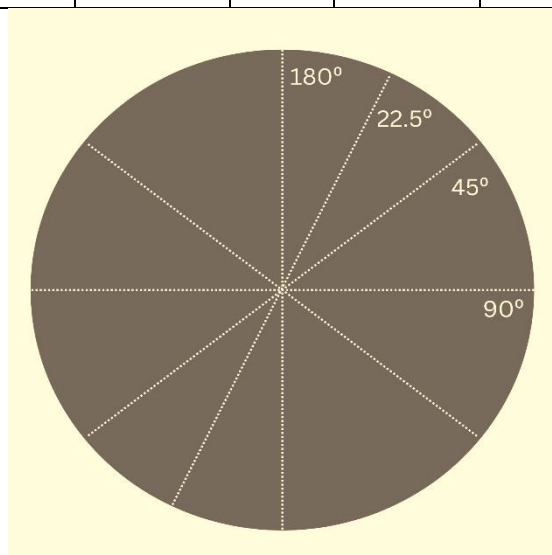


Figure 2.7: Folding Axes of the Hydrogel Film for Folding Endurance

The reaction optimization process involved making adjustments to the crosslinker amount, that is Citric acid in our HyPPGG-*co*-CaMGG-*cl*-CTA hydrogel film. The experiment took place at room temperature with the objective of minimizing the crosslinker amount while maximizing flexibility and strength of the film. Flexibility was assessed using the folding endurance method, which measures the number of folds achievable after film formation. To simplify study procedures, circular films were created for all variations due to their symmetry which ensured that folding lines coincided with circular axes, facilitating identification of folding paths. The optimization results uncovered that ideal films with minimal crosslinker and maximum flexibility are those with Gums:CTA ratios of 1:0.4 (R3) and 1:0.6 (R4). It was observed that films with Folding Endurance equal to 1 broke upon a single fold as seen in R2, R8, R9, R10, and R11 iterations. Introducing glycerol as a plasticizer proved beneficial for enhancing film flexibility.

The R4 hydrogel film formulation was selected for further characterization because it demonstrated the highest folding endurance as shown in Table 2.1 and maximum swelling as depicted in Table 3.1 respectively.

CHAPTER 3
RESULTS AND DISCUSSION

3.1 FTIR Spectroscopy:

Analysing the functional groups in HyPGG, CaMGG, and HyPGG-co-CaMGG-*cl*-CTA were conducted within the range of 4000-400 cm^{-1} . Notable peaks were observed in HyPGG at distinct wavenumbers including 3348 cm^{-1} for stretching vibrations of O-H, 2924 cm^{-1} for C-H asymmetric stretching, 1647 cm^{-1} for bending vibrations of H-O-H, 1373 cm^{-1} in-plane bending vibrations of C-H, and 1018 cm^{-1} for stretching vibrations of C-O.[17]

Characteristic peaks can be observed in CaMGG at distinct wavenumbers such as 3368 cm^{-1} for O-H stretching vibrations. The reduced intensity of this peak is due to an upsurge in hydrogen bonding interactions resulting from the addition of carboxymethyl group (CH_2COOH). Another peak at 2930 cm^{-1} corresponds to asymmetric stretching of C-H bond. Moreover, the presence of peak at 1717 cm^{-1} indicates COO^- asymmetric stretching vibrations while peaks at 1593 cm^{-1} and 1388 cm^{-1} represent COO^- symmetric stretching vibrations.[18]

HyPGG-*co*-CaMGG-*cl*-CTA shows characteristic peaks at specific wavenumbers, such as 3355 cm^{-1} which associate to the O-H stretching frequency. The intensity of this peak is diminished because of the reduction of O-H substituents upon crosslinking with Citric Acid. The peak at 2940 cm^{-1} correlate to C-H asymmetric stretch that exhibits reduced intensity as compared to HyPGG and CaMGG. Additionally, the peak showed up at 1720 cm^{-1} correspond to the carbonyl (C=O) bond of the free carboxylic acid and the ester linkage. Increased intensity of the peak is an indication of the crosslinking of citric acid with the free O-H groups resulting in ester linkages.[19]

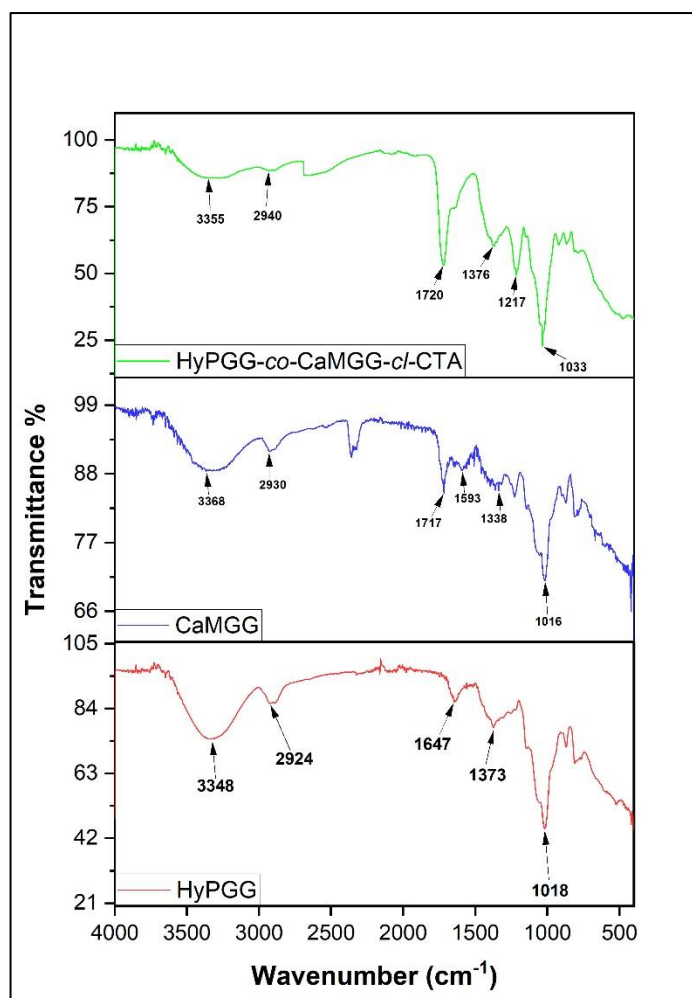


Figure 3.1: FTIR Spectra of HyPPG, CaMGG, HyPPG-co-CaMGG-cl-CTA hydrogel film

3.2 X-Ray Diffraction (XRD) Analysis:

The X-Ray Diffraction results yield vital insights into how the composition impacts the formation of crystal structure and morphology. The X-ray diffraction patterns were obtained for CA, HyPPG, CaMGG, and HyPPG-co-CaMGG-cl-CTA.

Citric Acid displays a crystalline structure, characterized by prominent peaks at specific angles: 13.92°, 16.35°, 17.94°, 24.72°, 33.25°, and 43.03°. These values confirm the crystalline nature of Citric Acid.[20]

Powdered HyPPG exhibited a distinct X-Ray Diffractogram with a peak 2θ at 20.12° , indicating the relatively lower amorphous nature of the hydroxypropyl group in HyPPG. Powdered CaMGG displayed a broad peak at $2\theta = 20.06^\circ$, suggesting its crystalline properties. Additionally, the distinct sharp peaks observed in CaMGG at specific 2θ angles are attributed to the characteristic carboxymethylation in CaMGG.[18]

The X-ray diffractogram revealed a broad peak at $2\theta = 17.94^\circ$, indicating the amorphous nature of HyPPG-co-CaMGG-cl-CTA. The crosslinking of citric acid with the co-polymerized HyPPG and CaMGG led to the formation of an even more amorphous structure, as evident from the disappearance of specific sharp characteristic peaks associated with CA and CaMGG.

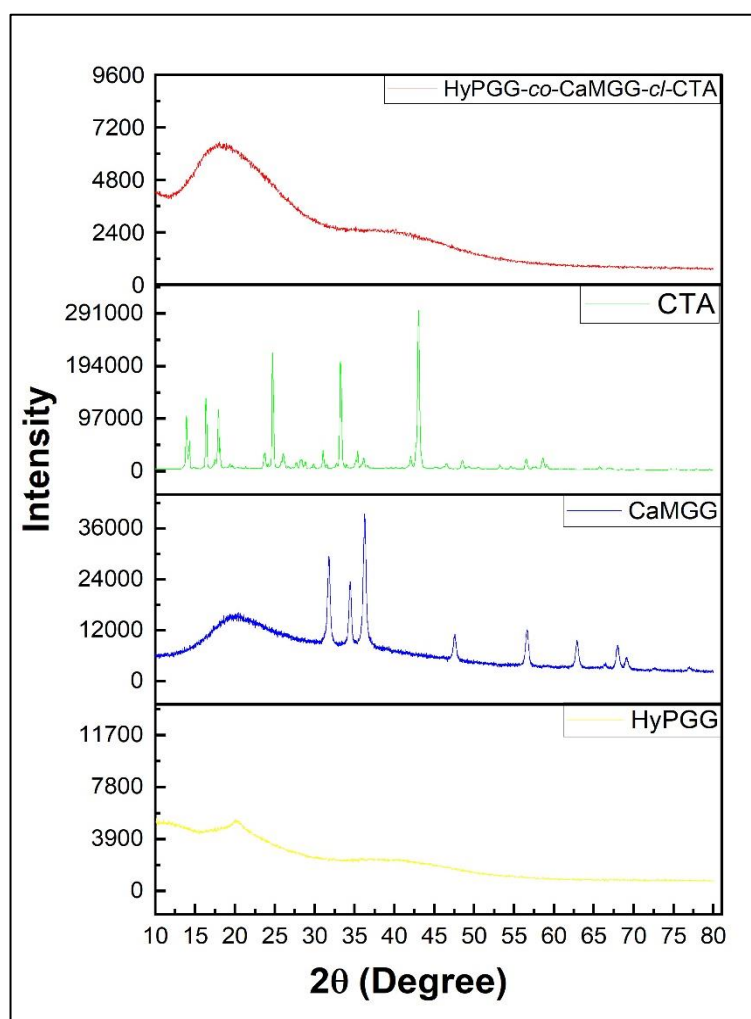


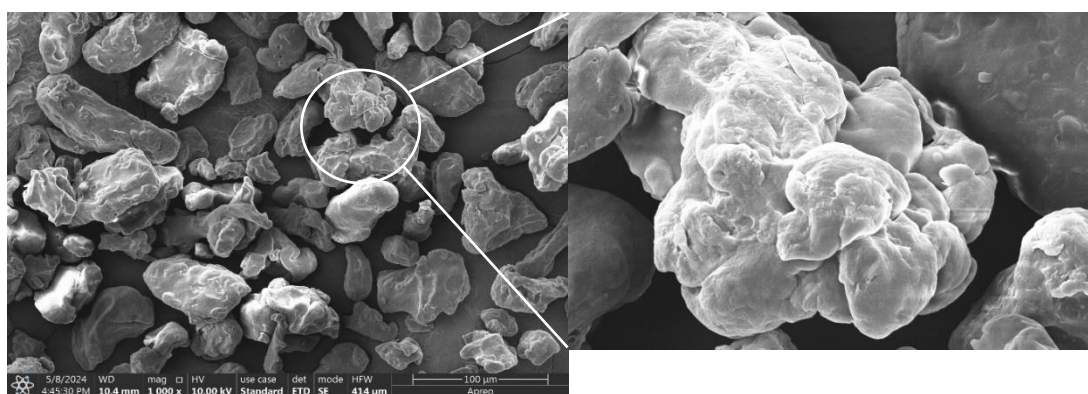
Figure 3.2: XRD Spectra of HyPPG, CaMGG, HyPPG-co-CaMGG-cl-CTA hydrogel film.

3.3 Scanning Electron Microscopy (SEM) Analysis:

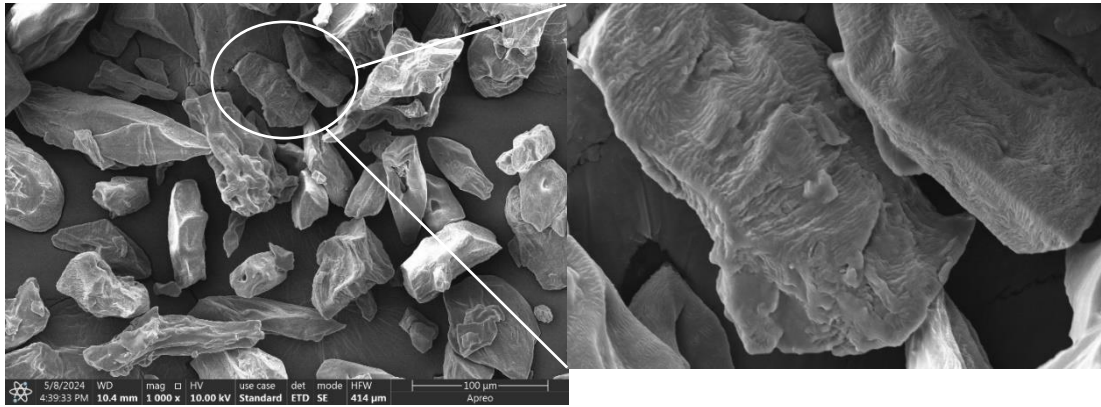
Scanning Electron Microscopy (SEM) images of HyPGG, CaMGG, and the HyPGG-co-CaMGG-cl-CTA hydrogel were captured at varying magnifications. SEM has proven to be highly valuable in assessing and confirming structural characteristics.[21]

SEM analysis of HyPGG and CaMGG reveals their granular appearance, with some granules adhering to each other. Notably, the HyPGG exhibits long irregular polygonal structures with rounded edges, while the irregular structures in CaMGG feature pointed edges. Both powdered forms display a distinct globular structure characterized by visible surface irregularities and aggregation.[22]

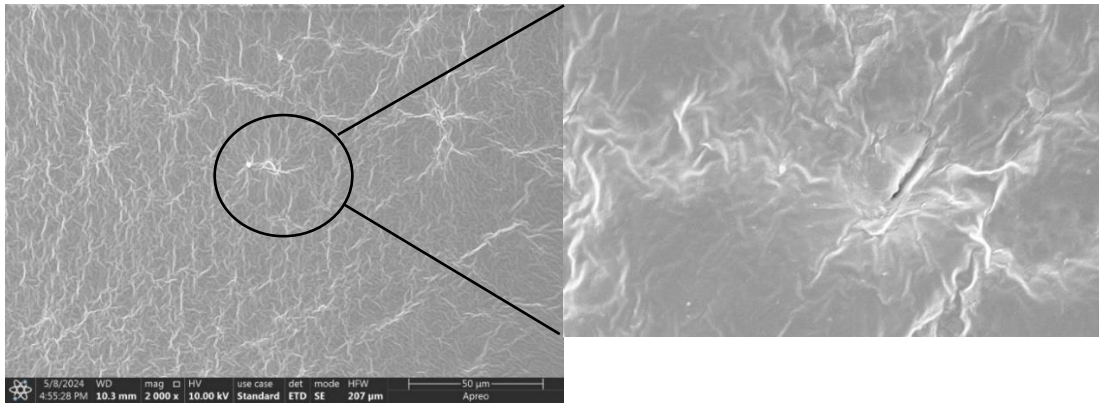
The SEM images of the HyPGG-co-CaMGG-cl-CTA hydrogel film displayed a distinct morphology in contrast to the individual HyPGG and CaMGG. The crosslinked hydrogel exhibited an interconnected and porous structure, offering a larger surface area compared to its individual components. Furthermore, the internal structure of the hydrogel film appeared compact and uniform with varied interlinking, enhancing its capacity for successful swelling and drug loading as well as release permeability.[23]



(A) SEM Image of Hydroxypropyl Guar Gum (HyPGG)



(B) SEM Images of Carboxymethyl Guar Gum (CaMGG)



(C) SEM Images of HyPPG-co-CaMGG-cl-CTA Hydrogel Film

Figure 3.3: Scanning Electron Micrographs of (A) HyPPG, (B) CaMGG and, (C) HyPPG-co-CaMGG-cl-CTA hydrogel film at 1000, 2000 and 5000 magnifications respectively

3.4 Thermogravimetric Analysis (TGA):

The graphical representation illustrates the Thermogravimetric Analysis findings for XHyPPG, CaMGG, and HyPPG-co-CaMGG-cl-CTA hydrogel film. In order to accommodate weight loss linked to trapped moisture, we utilized the initial decomposition temperature for each sample.

HyPPG underwent a three-stage degradation process, starting with an initial weight reduction of 10.922% between 35.2°C and 147.8°C due to moisture loss from the gum. The second stage, occurring from 147.8°C to 358.5°C, resulted in a weight loss of 55.912%, signifying the decomposition of polysaccharide

rings respectively. Finally, the third stage took place between 358.5°C to 470-8 °C resulting in a weight loss of 20.841% indicating breakdown of HyPPG's backbone. 12.325 composed of the residual weight.

CaMGG experienced a sequential degradation process. It displayed an initial mass reduction of 12.875% between the temperature bracket of 38.64°C to 148.48°C, attributed to moisture loss from the gum. The second phase, spanning from 148.39°C to 349.21°C, resulted in a weight loss of 44.917%, indicating the decomposition of polysaccharide rings respectively. The third stage occurred between 349–470°C with a weight loss percentage of 20.841% respectively. This is believed to signify the breakdown of CaMGG's backbone structure.

The hydrogel film HyPPG-*co*-CaMGG-*cl*-CTA exhibited a degradation process consisting of three distinct steps. The first step resulted in an initial weight reduction of 6.613% within the temperature range of 32.5°C to 103.74°C, followed by a second weight loss of 65.666% observed between 103.74°C and 394.75°C, and ultimately a third weight decrease of 4.752% occurring within the temperature range of 394.75°C to 496.54°C.

These results suggest that the heat resistance of gums like HyPPG and CaMGG diminishes as they go through the decomposition stages. Nevertheless, when combined in the HyPPG-*co*-CaMGG-*cl*-CTA hydrogel film, copolymerization and film formation processes show improved stability and resilience against thermal degradation compared to each gum individually.[24]

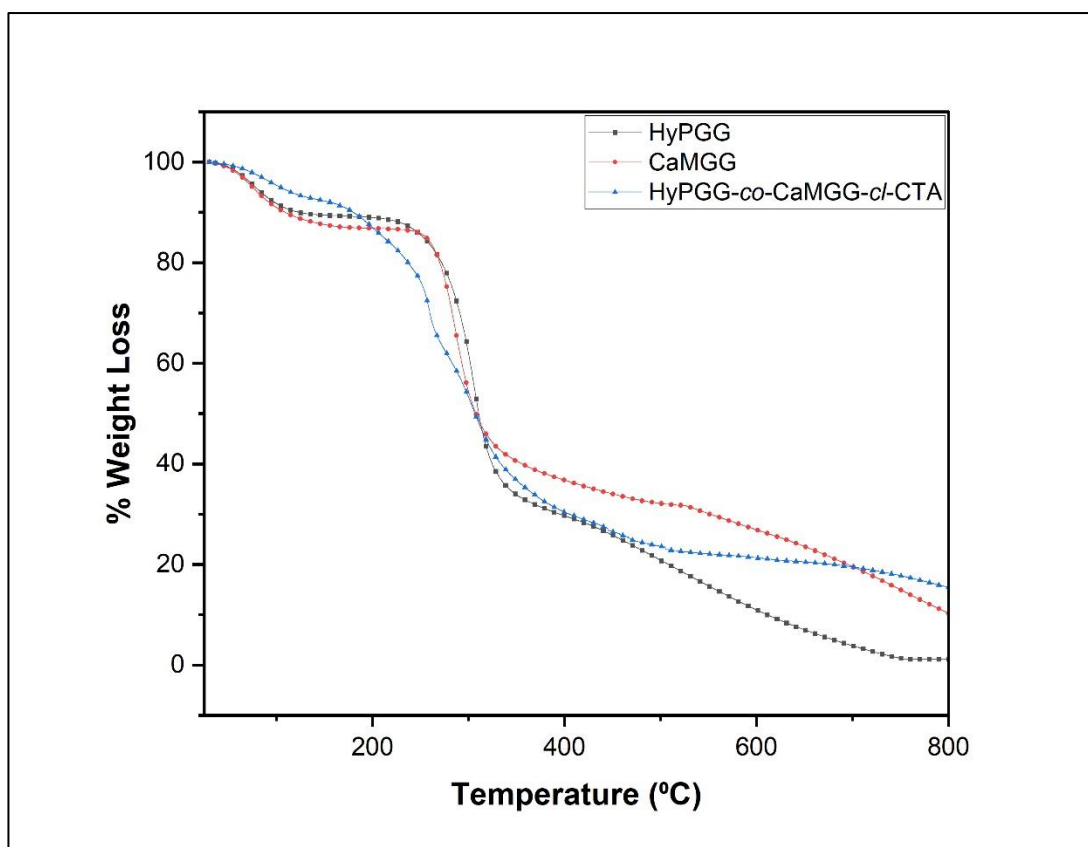


Figure 3.4: Thermogravimetric Analysis of HyPGG, CaMGG and HyPGG-co-CaMGG-cl-CTA hydrogel film a heating rate of 10°C/min in an N₂ atmosphere

3.5 Rheological Analysis

D) Viscosity:

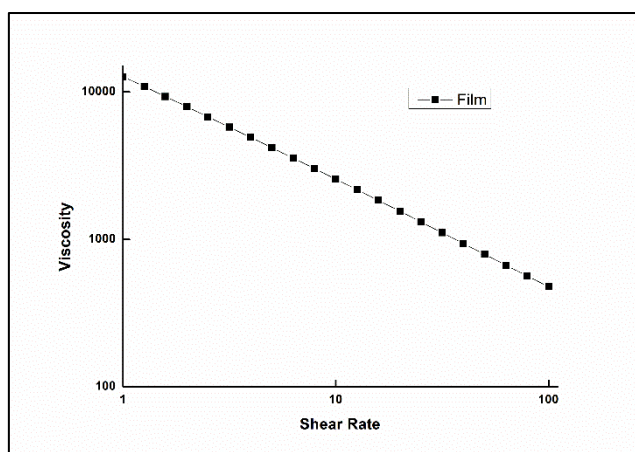
Rheology is the scientific discipline that examines how materials respond to deformation and flow, investigating the connection between force, deformation, and time. It encompasses experimental techniques for studying and assessing the rheological characteristics of different substances. Shear rheological analysis involved adjusting the shear rate from $10s^{-1}$ to $102s^{-1}$. The outcomes revealed that solution of HyPGG-co-CaMGG-cl-CTA displayed a decrease in viscosity due to shear thinning behaviour as shown in the Figure 3.5 (A). This reduction was attributed to the alignment of HyPGG-co-CaMGG-cl-CTA induced by shear forces in the direction of flow.

II) Amplitude Sweep:

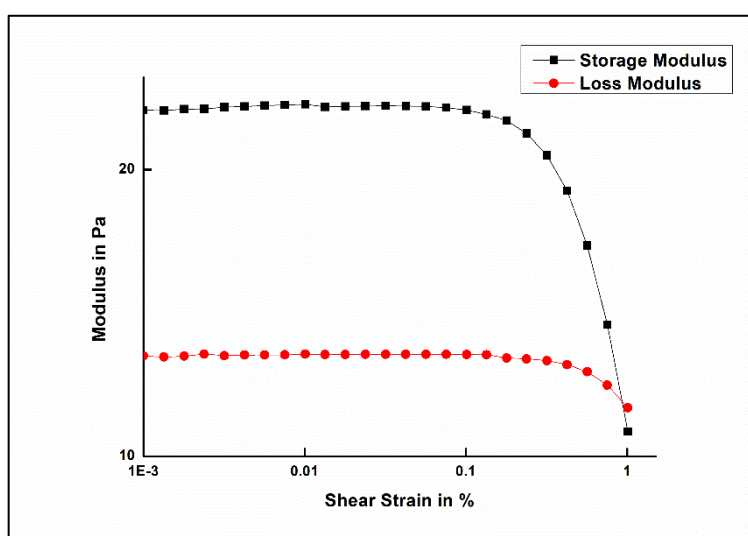
A test was conducted to analyse the linear viscoelastic range and evaluate the structural and mechanical stability of the hydrogel. This assessment helped establish both upper and lower limits of the LVE range. A graph was generated to display the storage modulus and loss modulus (G'') in relation to shear strain percentage, as shown in Figure 3.5(B). The results revealed that within this linear viscoelastic region, the storage modulus remained consistent at low deformation, signifying stable sample structure. At lower strains, HyPPGG-*co*-CaMGG-*cl*-CTA exhibited characteristics of a viscoelastic solid material; however, at higher strains it displayed properties akin to a viscoelastic fluid due to structural disruption – marking an end to its linear viscoelastic behaviour. The plateau value of G' within this LVE region reflects inherent rigidity in the sample material (22.9 Pa for HyPPGG-*co*-CaMGG-*cl*-CTA). When reaching this endpoint, approximately 80% of its initial shear modulus value had been retained - typically indicating peak solidity for such samples under these conditions - with a critical value (γ_c) found at 13%.

III) Frequency Sweep:

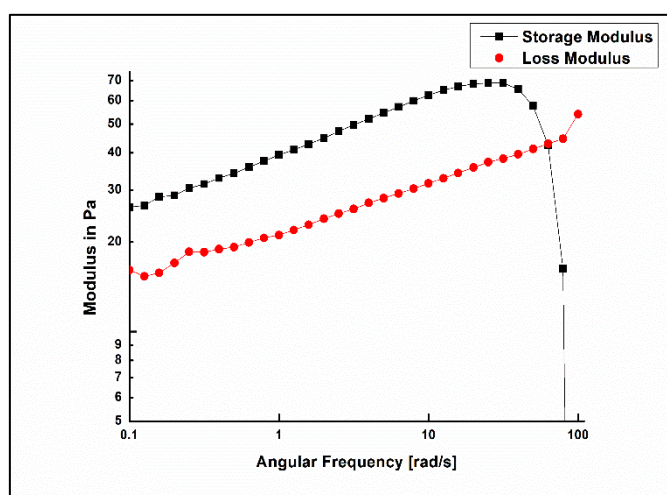
The frequency sweep test evaluates the viscoelastic properties of a material by analysing the changes in G' and G'' across different frequencies. Studies show that by introducing additives and found that all hydrogels displayed viscoelastic behaviour, with both G' and G'' showing positive slopes. During the test, shear strain percentage was kept constant within the linear viscoelastic region while frequency varied from 1 to 100 rad/s. The results indicated that in HyPPGG-*co*-CaMGG-*cl*-CTA solution, loss modulus (G'') dominates at high frequencies, while storage modulus is predominant at low frequencies – pointing to a viscoelastic solid behaviour as shown in Figure 3.5(C).



A



B



C

Figure 3.5: Rheological Studies of HyPGG-co-CaMGG-cl-CTA solution: (A) Shear Viscosity of HyPGG-co-CaMGG-cl-CTA solution, (B) Amplitude Sweep of HyPGG-co-CaMGG-cl-CTA solution, (C) Frequency Sweep of HyPGG-co-CaMGG-cl-CTA solution

3.6 Swelling Studies of the Hydrogel Film:

The graph illustrates the findings of the swelling studies. It is evident from the visual representation that nearly all films exhibited a similar rate of swelling in the initial 60 minutes after the commencement of the studies. The extent of cross-linking has a substantial impact in influencing the swelling rate of hydrophilic matrix structures when dry scaffold films come into contact with PBS 7.4. Throughout the study period, R3 and R4 films consistently absorbed PBS solution and maintained their volumes until reaching the 24-hour mark, while R8, R9, R10, and R11 showed a decreasing trend. The highest swelling equilibrium (80.4305%) was observed in film R4 with a Gums to CTA ratio of 1:0.6, whereas film R11 with a Gums to CTA ratio of 1:2 recorded the lowest equilibrium swelling ratio (71.831%). It can be concluded that an increase in Citric Acid concentrations led to decreased swelling ratios in scaffold films due to increased porosity resulting from sufficiently cross-linked films forming porous structures like those seen in batched film 'R11'. In contrast, more un-crosslinked gums present in 'R4' batch's films resulted in less porous structures possibly causing increased swelling ratios. Given that temperature, time, and gum concentration were consistent across all batches, the differences are minimal depicting little variation among different batches' trends towards swellings.

TABLE 3.1: Swelling Index of different formulations by varying the concentration of CTA

Sample Code	Ratio (Gums: CTA)	Swelling Index (%)
R1	1:0	None
R2	1:0.2	351
R3	1:0.4	385
R4	1:0.6	411
R5	1:0.8	361
R6	1:1	338
R7	1:1.2	329
R8	1:1.4	293
R9	1:1.6	269
R10	1:1.8	261
R11	1:2	255

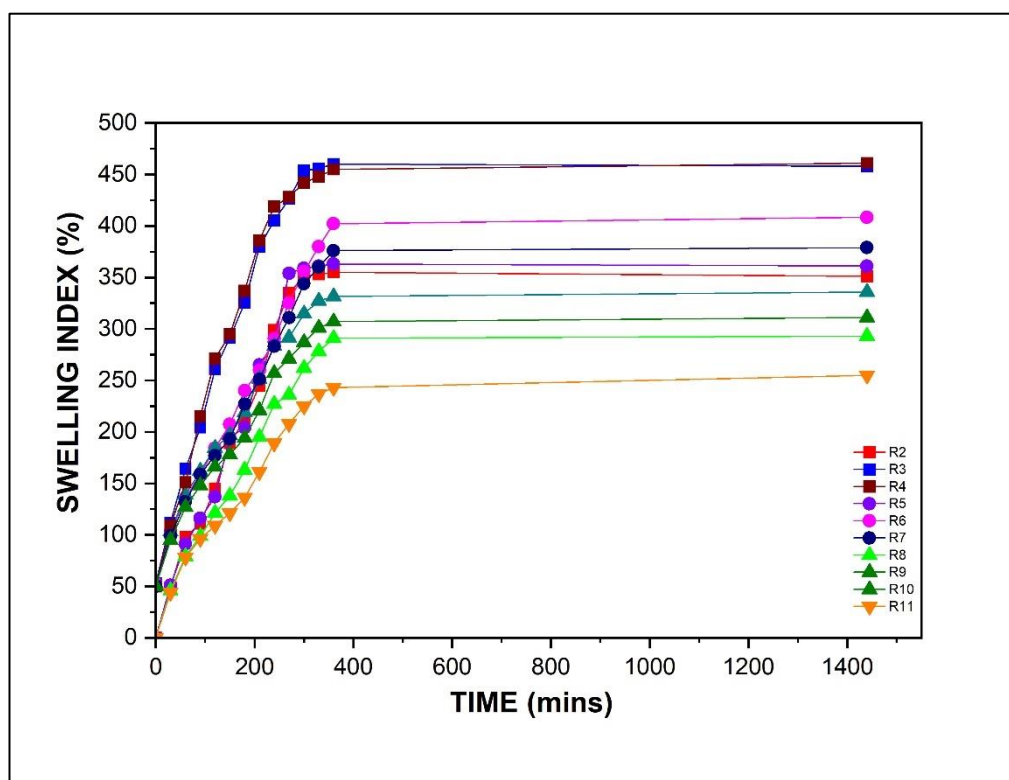


Figure 3.6 Graph of swelling Index different formulations by varying the concentration of CTA

CHAPTER 4
DRUG DELIVERY APPLICATION

The research illustrated the potential for utilizing the created HyPGG-*co*-CaMGG-*cl*-CTA hydrogel films in controlled drug delivery. Piroxicam was incorporated into the hydrogel matrix and the *in vitro* release study was done at regular intervals of time for a certain time period.

The drug encapsulation of the HyPGG-*co*-CaMGG-*cl*-CTA hydrogel film formulation R4 was determined due to its significant swelling behaviour. PXM loaded hydrogel film with 0.1g was placed into 50 ml of Phosphate Buffer Solution, pH 7.4 and the incubation was performed for 24 hours. The solution was further tested with a UV-Vis spectrophotometer to test absorbance at λ_{\max} 351 nm.

4.1 *In-Vitro* Release of Piroxicam

In-vitro studies were undertaken to analyse the potential of the prepared hydrogel films in delivering PXM. The release of PXM loaded HyPGG-*co*-CaMGG-*cl*-CTA hydrogel film (R4) was examined at pH 7.4, chosen for its optimal swelling properties. Samples were collected at regular intervals and replaced with fresh buffer solution before being assessed using a UV spectrophotometer at λ_{\max} 351 nm to determine drug release through calibration curve analysis.

The *in-vitro* study analysed the release of PXM from a specific hydrogel film (R4) over 24 hours in PBS at pH 7.4. The highest observed release of PXM was 73.59% within the timeframe of 24 hours, indicating an increased swelling ratio that enhances drug loading and release capability. This suggests that the HyPGG-*co*-CaMGG-*cl*-CTA hydrogel film could be suitable for controlled drug release applications.

4.2 Kinetic Modelling of Piroxicam

Different drug release models like Zero order, Hixson–Crowell, Korsmeyer– Peppas, Higuchi and First-Order models were used to understand the drug release patterns of the PXM loaded HyPGG-*co*-CaMGG-*cl*-CTA hydrogel film. An appropriate model was chosen with the consideration in the value of "R²" being close to 1. The values of the release exponent "n" show the drug release mechanism.

The findings indicate that the drug release from the hydrogel is linked to the swelling of the hydrogel and adheres to the Fickian mechanism. The kinetics underwent further examination through fitting the drug release data to various mathematical models. Notably, the Korsmeyer-Peppas model exhibited a high correlation coefficient (R^2) value, signifying drug release from a polymeric system. The 'n' value measured at 0.3499 in table supports this, as it is less than 0.5 and aligns with the Fickian mechanism of diffusion-controlled drug release driven by a chemical gradient. Additionally, results from the Higuchi model also corroborate Fickian diffusion of drugs from within the hydrogel's polymeric matrix.

TABLE 4.1: Kinetic Modelling data of PXM release from HyPGG-co-CaMGG-cl-CTA hydrogel film

Model	Equation	n	R ²
Zero -Order	$W_t = W_\infty + W_{0t}$		0.8415
First Order	$\text{Log}W_t = \text{Log}W_\infty + kt/2.303$, where k=rate constant		0.7848
Higuchi	$F = W_t / W_\infty = k_H t^{1/2}$, where k_H =kinetic constant		0.9807
Hixson-Crowell	$(W_0)^{1/3} - (W_t)^{1/3} = k_{HC}.t$, where k_{HC} = Hixson-Crowell constant		0.7459
Korsmeyer-Peppas	$F = W_t / W_\infty = kt^n$, where k= kinetic constant, n= diffusion exponent Fickian diffusion ($n < 0.5$) Non-Fickian diffusion ($0.89 > n > 0.5$) Case II Transport ($n > 0.89$)	0.3499	0.9902

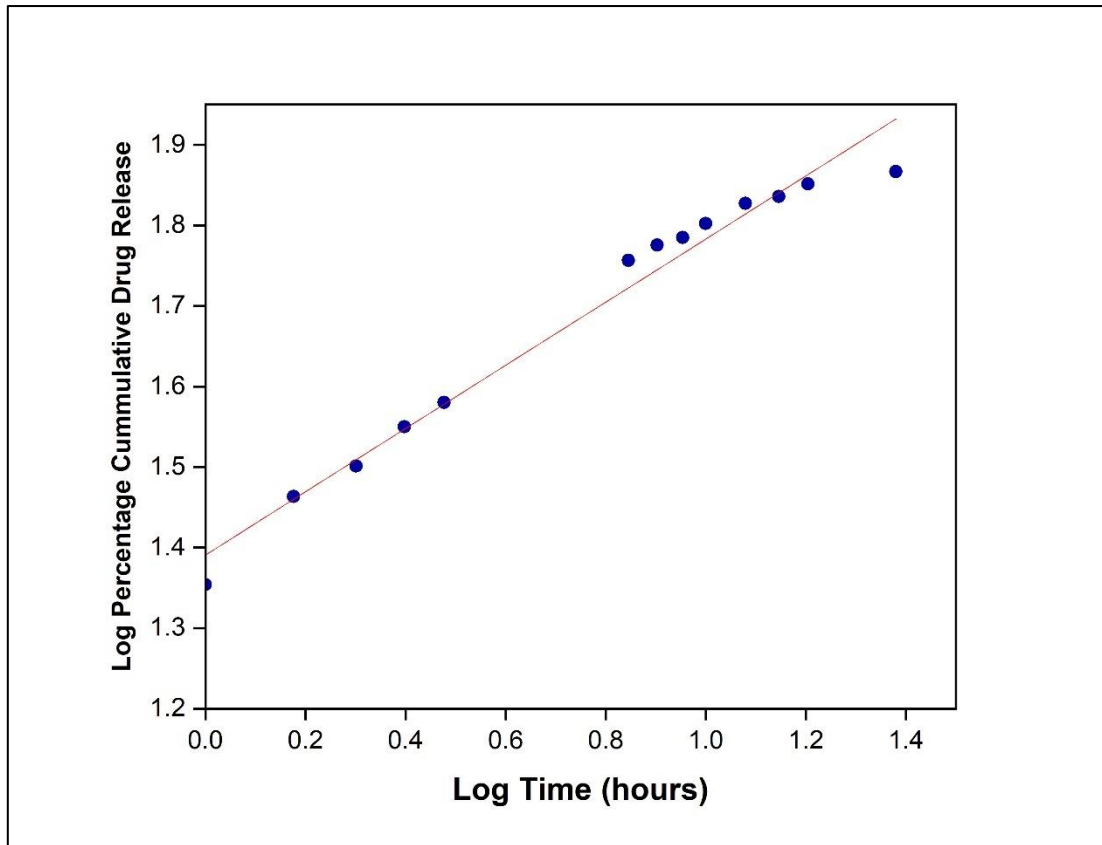


Figure 4.1: Release kinetic of Piroxicam in accordance with the Korsmeyer-Peppas Model in pH 7.4

CONCLUSION

To conclude, HyPGG-co-CaMGG-cl-CTA hydrogel film was developed through copolymerization reaction mechanism. A Piroxicam-loaded derivative was synthesized to explore drug release kinetics for potential use in drug delivery systems. The unloaded hydrogel was then characterized using various techniques such as ATR-FTIR, XRD, FE-SEM, and TGA. FT-IR analysis for the hydrogel film suggested that the diminished intensity of the O-H peak (3355 cm^{-1}) is due to the crosslinking of gums with citric acid in the hydrogel film. X-Ray Diffraction analysis suggested the amorphous nature of the hydrogel film with $2\theta = 17.94^\circ$. FE-SEM images were taken at magnifications of 2000x and 5000x suggesting a closed morphology of the film subjected to crosslinking. Thermogravimetric studies provided information on thermal stability of the hydrogel film and suggested to have increased heat resistance due to crosslinking. Rheological studies showed shear thinning behaviour which resulted in decrease in viscosity. Amplitude sweep of hydrogel films showed a viscoelastic behaviour at lower strains and a similar viscoelastic fluid behaviour was observed at higher strains. Frequency Sweep showed that loss modulus subjected at higher frequencies while storage modulus was prominent at lower frequencies suggesting the viscoelastic behaviour of the film. Furthermore, the impact of CTA amount on the swelling ratio of the developed hydrogel film was investigated. The R4 formulation of the hydrogel film exhibited highest swelling in 24 hours when dipped in PBS 7.4. *In-vitro* analysis revealed that under pH 7.4 conditions, release kinetics adhered well to the Korsmeyer–Peppas model and followed a Fickian mechanism of diffusion at this pH level. This indicates potential applicability of HyPGG-co-CaMGG-cl-CTA hydrogel film as a carrier for innovative drug delivery systems.

REFERENCES

- [1] A. Umamaheswari, M. Vijayalakshmi, S. B. Raj, D. K. Chellappan, and S. L. Prabu, "Gum-Based Drug Delivery Systems," in *Natural Polymeric Materials based Drug Delivery Systems in Lung Diseases*, Singapore: Springer Nature Singapore, 2023, pp. 147–166. doi: 10.1007/978-981-19-7656-8_8.
- [2] S. Ahmad, M. Ahmad, K. Manzoor, R. Purwar, and S. Ikram, "A review on latest innovations in natural gums based hydrogels: Preparations & applications," *International Journal of Biological Macromolecules*, vol. 136. Elsevier B.V., pp. 870–890, Sep. 01, 2019. doi: 10.1016/j.ijbiomac.2019.06.113.
- [3] S. Dhar, E. Maheswara Reddy, A. Shiras, V. Pokharkar, and B. L. V. Prasad, "Natural gum reduced/stabilized gold nanoparticles for drug delivery formulations," *Chemistry - A European Journal*, vol. 14, no. 33, pp. 10244–10250, Nov. 2008, doi: 10.1002/chem.200801093.
- [4] A. Abrar, S. Yousuf, and M. K. Dasan, "Formulation and evaluation of microsphere of antiulcer drug using Acacia nilotica gum.," *Int J Health Sci (Qassim)*, vol. 14, no. 2, pp. 10–17, 2020.
- [5] S. C. Viñarta, N. J. François, M. E. Daraio, L. I. C. Figueroa, and J. I. Fariña, "Sclerotium rolfii scleroglucan: The promising behavior of a natural polysaccharide as a drug delivery vehicle, suspension stabilizer and emulsifier," *Int J Biol Macromol*, vol. 41, no. 3, pp. 314–323, Aug. 2007, doi: 10.1016/j.ijbiomac.2007.04.001.
- [6] S. Barak, D. Mudgil, and S. Taneja, "Exudate gums: chemistry, properties and food applications – a review," *Journal of the Science of Food and Agriculture*, vol. 100, no. 7. John Wiley and Sons Ltd, pp. 2828–2835, May 01, 2020. doi: 10.1002/jsfa.10302.
- [7] A. George, P. A. Shah, and P. S. Shrivastav, "Guar gum: Versatile natural polymer for drug delivery applications," *European Polymer Journal*, vol. 112. Elsevier Ltd, pp. 722–735, Mar. 01, 2019. doi: 10.1016/j.eurpolymj.2018.10.042.
- [8] N. Thombare, U. Jha, S. Mishra, and M. Z. Siddiqui, "Guar gum as a promising starting material for diverse applications: A review," *Int J Biol Macromol*, vol. 88, pp. 361–372, Jul. 2016, doi: 10.1016/j.ijbiomac.2016.04.001.
- [9] M. Prabakaran, "Prospective of guar gum and its derivatives as controlled drug delivery systems," *International Journal of Biological Macromolecules*, vol. 49, no. 2. Elsevier B.V., pp. 117–124, 2011. doi: 10.1016/j.ijbiomac.2011.04.022.
- [10] D. Mudgil, S. Barak, and B. S. Khatkar, "Guar gum: Processing, properties and food applications - A Review," *Journal of Food Science and Technology*, vol. 51, no. 3. pp. 409–418, Mar. 2014. doi: 10.1007/s13197-011-0522-x.
- [11] L. Zhou, Z. Xu, J. Zhang, Z. Zhang, and Y. Tang, "Degradation of hydroxypropyl guar gum at wide pH range by a heterogeneous Fenton-like process using bentonite-

supported Cu(0)," *Water Science and Technology*, vol. 82, no. 8, pp. 1635–1642, Oct. 2020, doi: 10.2166/wst.2020.436.

- [12] H. Gong, M. Liu, J. Chen, F. Han, C. Gao, and B. Zhang, "Synthesis and characterization of carboxymethyl guar gum and rheological properties of its solutions," *Carbohydr Polym*, vol. 88, no. 3, pp. 1015–1022, Apr. 2012, doi: 10.1016/j.carbpol.2012.01.057.
- [13] G. Dalei and S. Das, "Carboxymethyl guar gum: A review of synthesis, properties and versatile applications," *European Polymer Journal*, vol. 176. Elsevier Ltd, Aug. 05, 2022. doi: 10.1016/j.eurpolymj.2022.111433.
- [14] G. Dodi *et al.*, "Carboxymethyl guar gum nanoparticles for drug delivery applications: Preparation and preliminary in-vitro investigations," *Materials Science and Engineering C*, vol. 63, pp. 628–636, Jun. 2016, doi: 10.1016/j.msec.2016.03.032.
- [15] M. J. Tavera-Quiroz, J. Feria Díaz, and A. Pinotti, "Characterization of Methylcellulose Based Hydrogels by Using Citric Acid as a Crosslinking Agent," 2018. [Online]. Available: <http://www.ripublication.com>
- [16] J. Jose and M. A. Al-Harhi, "Citric acid crosslinking of poly(vinyl alcohol)/starch/graphene nanocomposites for superior properties," *Iranian Polymer Journal (English Edition)*, vol. 26, no. 8, pp. 579–587, Aug. 2017, doi: 10.1007/s13726-017-0542-0.
- [17] D. Mudgil, S. Barak, and B. S. Khatkar, "X-ray diffraction, IR spectroscopy and thermal characterization of partially hydrolyzed guar gum," *Int J Biol Macromol*, vol. 50, no. 4, pp. 1035–1039, May 2012, doi: 10.1016/j.ijbiomac.2012.02.031.
- [18] A. Rahmatpour and N. Alijani, "An all-biopolymer self-assembling hydrogel film consisting of chitosan and carboxymethyl guar gum: A novel bio-based composite adsorbent for Cu²⁺ adsorption from aqueous solution," *Int J Biol Macromol*, vol. 242, Jul. 2023, doi: 10.1016/j.ijbiomac.2023.124878.
- [19] P. Orsu and S. Matta, "Fabrication and characterization of carboxymethyl guar gum nanocomposite for application of wound healing," *Int J Biol Macromol*, vol. 164, pp. 2267–2276, Dec. 2020, doi: 10.1016/j.ijbiomac.2020.07.322.
- [20] M. Todica, M. Muresan-Pop, C. Niculaescu, and M. Constantiniuc, "XRD AND FTIR INVESTIGATION OF THE STRUCTURAL CHANGES OF THE HUMAN TOOTH INDUCED BY CITRIC ACID," 2020.
- [21] M. M. Horn, V. C. A. Martins, and A. M. de Guzzi Plepis, "Influence of collagen addition on the thermal and morphological properties of chitosan/xanthan hydrogels," *Int J Biol Macromol*, vol. 80, pp. 225–230, Jul. 2015, doi: 10.1016/j.ijbiomac.2015.06.011.
- [22] M. Dogan, D. Aslan, and V. Gurmeric, "The rheological behaviors and morphological characteristics of different food hydrocolloids ground to sub-micro particles: in terms of temperature and particle size," *Journal of Food Measurement and*

Characterization, vol. 12, no. 2, pp. 770–780, Jun. 2018, doi: 10.1007/s11694-017-9691-2.

- [23] Y. Luo, K. R. Kirker, and G. D. Prestwich, “Cross-linked hyaluronic acid hydrogel films: new biomaterials for drug delivery,” 2000. [Online]. Available: www.elsevier.com/locate/jconrel
- [24] B. Singh and N. Sharma, “Mechanistic implication for cross-linking in sterculia-based hydrogels and their use in GIT drug delivery,” *Biomacromolecules*, vol. 10, no. 9, pp. 2515–2532, Sep. 2009, doi: 10.1021/bm9004645.